Neutron Spin Resonance in a Quasi-Two-Dimensional Iron-Based Superconductor

Wenshan Hong,[1,2] Linxing Song,[1,2] Bo Liu,[1,2] Zezong Li,[1,2] Zhenyuan Zeng,[1,2] Yang Li,[1,2] Dingsong Wu,[1,2] Qiangtao Sui,[1,2] Tao Xie,[1,2] Sergey Danilkin,[3] Haranath Ghosh,[4,5] Abyay Ghosh,[4,5] Jiangping Hu,[1,2,6] Lin Zhao,[1,6] Xingjiang Zhou,[1,2,6] Xianggang Qiu,[1,2,6] Shiliang Li,[1,2,6,*] and Huiqian Luo[1,6,†]

[1]*Beijing National Laboratory for Condensed Matter Physics, Institute of Physics, Chinese Academy of Sciences, Beijing 100190, China*
[2]*University of Chinese Academy of Sciences, Beijing 100049, China*
[3]*Australian Centre for Neutron Scattering, Australian Nuclear Science and Technology Organization, Lucas Heights NSW-2234, Australia*
[4]*Human Resources Development Section, Raja Ramanna Centre for Advanced Technology, Indore 452013, India*
[5]*Homi Bhabha National Institute, BARC training school complex, Anushakti Nagar, Mumbai 400094, India*
[6]*Songshan Lake Materials Laboratory, Dongguan, Guangdong 523808, China*

(Received 11 June 2020; revised 2 August 2020; accepted 17 August 2020; published 10 September 2020)

The neutron spin resonance is generally regarded as a key to understanding the magnetically mediated Cooper pairing in unconventional superconductors. Here, we report an inelastic neutron scattering study on the low-energy spin excitations in a quasi-two-dimensional iron-based superconductor $KCa_2Fe_4As_4F_2$. We have discovered a two-dimensional spin resonant mode with downward dispersions, a behavior closely resembling the low branch of the hourglass-type spin resonance in cuprates. While the resonant intensity is predominant by two broad incommensurate peaks near $Q = (0.5, 0.5)$ with a sharp energy peak at $E_R = 16$ meV, the overall energy dispersion of the mode exceeds the measured maximum total gap $\Delta_{\mathrm{tot}} = |\Delta_k| + |\Delta_{k+Q}|$. These results deeply challenge the conventional understanding of the resonance modes as magnetic excitons regardless of underlining pairing symmetry schemes, and it also points out that when the iron-based superconductivity becomes very quasi-two-dimensional, the electronic behaviors are similar to those in cuprates.

DOI: 10.1103/PhysRevLett.125.117002

In copper-oxide [1,2], heavy-fermion [3,4], iron-pnictide and iron-chalcogenide superconductors [5–7], a neutron spin resonance is intensively observed in the superconducting state. This collective mode is born from the dynamic spin susceptibility $\chi''(Q, \omega)$ already present in the normal state, and its intensity changes with temperature like the superconducting order parameter [8–10]. More importantly, the mode energy E_R seems linearly related to either T_c or the superconducting gap [11–16], hinting a universal magnetic origin of the Cooper pairings in unconventional superconductors analogous to the phonon mediated conventional superconductivity [17–19].

Although many theories have been proposed to explain the spin resonance in unconventional superconductors, the most successful candidate until now is the so-called spin-exciton scenario [10,11]. Namely, the spin resonance is a spin-1 exciton from the collective particle-hole excitations below a spin-flip continuum energy $\hbar\omega_c$, which should be slightly lower than twice the superconducting gap (pair-breaking gap) 2Δ. Thus, the dispersion of spin resonance is determined by the momentum dependence of the spin fluctuations and simultaneously limited by the continuum threshold $\hbar\omega_c$. In the single-band d-wave superconductors like cuprates, as the gap magnitude is strongly momentum dependent from the antinodal to nodal region, a downward dispersion of the resonance is observed beneath the dome of $\hbar\omega_c$ [10]. Together with the upward magnonlike dispersion at energies above E_R, they form hourglass-type spin excitations [Fig. 1(a)] [8,11]. While the case in iron-based superconductors (FeSCs) is complicated for its multiband nature, and the spin resonance is regarded as the hallmark of sign-reversed $s^{\pm}$-wave pairings on the Fermi surfaces connected by a finite wave vector Q [20–28]. In this case, $\hbar\omega_c$ is defined by the total superconducting gap summed on two Fermi surfaces linked by Q: $\Delta_{\mathrm{tot}} = |\Delta_k| + |\Delta_{k+Q}|$, which is usually momentum independent. Thus, the resonance should reveal an upward magnon-like dispersion instead [Fig. 1(b)] [26–31]. Alternately, a resonancelike hump is also proposed in FeSCs under the conventional s^{++}-pairing picture due to the self-energy effect induced redistribution of spin fluctuations below T_c [32–35]. When the enhancement of dynamical spin susceptibility from self-energy exceeds the suppression due to the coherence factor effect in the superconducting state, the spin excitations may have a steep upward dispersion in momentum space [Fig. 1(c)] [36] and form a broad energy hump [Fig. 1(d)] above Δ_{tot} [34,35]. For comparison, a broad spin resonant peak below Δ_{tot} is predicted when d-wave pairings emerge on the hole pockets in the zone center [Fig. 1(d)] [29]. Experimentally,

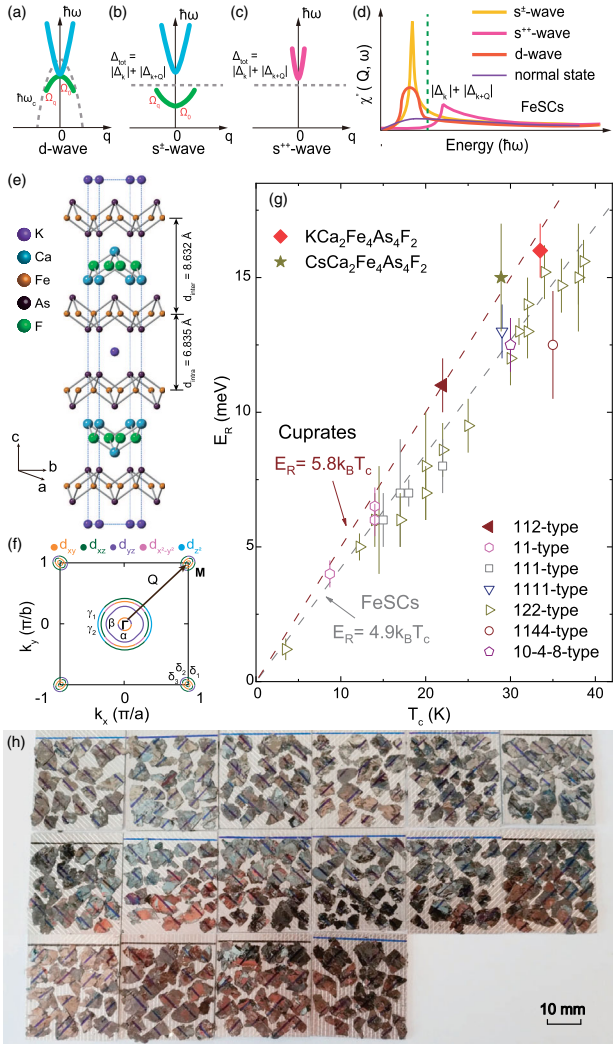

FIG. 1. (a)–(c) Dispersion of spin excitations and resonance under the pairing symmetries d wave in cuprates, $s^{\pm}$ wave and s^{++} wave in FeSCs. (d) Comparison between the spin resonant peak under $s^{\pm}/d$-wave pairing and spin-resonancelike hump under s^{++}-wave pairing in FeSCs. Here, $\hbar\omega_c$ (or Δ_{tot}) is the continuum threshold energy in cuprates (or FeSCs). (e) Crystal structure of $KCa_2Fe_4As_4F_2$. (f) DFT calculation results on the Fermi surfaces shown in the Brillouin zone of 2-Fe unit cell. There are four visible hole pockets with distinct sizes around Γ point ($\alpha, \beta, \gamma_1, \gamma_2$) and three small electron pockets ($\delta_{1,2,3}$) around the M point. Each of them consists of different orbitals such as d_{xy}, d_{xz}, d_{yz}, $d_{x^2-y^2}$, and d_{z^2}. (g) Summarized E_R versus T_c in iron-based superconductors, where the ratio $E_R = 4.9k_BT_c$ scales most of them, and $E_R = 5.8k_BT_c$ is usually used in cuprates. (h) Photo of the coaligned $KCa_2Fe_4As_4F_2$ crystals.

only upward dispersions of the spin resonances are observed in FeSCs until now [31,36–38], and E_R is usually beneath Δ_{tot} ($E_R/\Delta_{\mathrm{tot}} \approx 0.64$) [12,15,39], thus supporting the spin-exciton picture under $s^{\pm}$ pairing.

Here, in this Letter, we report an inelastic neutron scattering study on the low-energy spin excitations of $KCa_2Fe_4As_4F_2$ single crystals, a newly discovered FeSC with quasi-two-dimensional (quasi-2D) characters and $T_c = 33.5$ K [Figs. 1(e) and 1(f)] [40]. A spin resonant mode is found at $E_R = 16$ meV, giving a ratio $E_R/k_BT_c = 5.5$ close to that in cuprates ($E_R/k_BT_c = 5.8$) rather than other FeSCs where $E_R/k_BT_c = 4.9$ [Fig. 1(g)] [11,41]. Surprisingly, the resonant intensity is 2D in reciprocal space and predominant by two broad incommensurate peaks near $Q = (0.5, 0.5)$, forming a downward dispersion with overall energy above the maximum total gap Δ_{tot}. These results demonstrate the commonality on the magnetism and superconductivity in both high-T_c families when their nature is very quasi-2D, but challenge those popular scenarios of the spin resonance.

High quality single crystals of $KCa_2Fe_4As_4F_2$ were grown by the self-flux method [42–44]. About 2.1 grams (~950 pieces) of crystals were coaligned by hydrogen-free glue on aluminum plates [see Fig. 1(h), some of them are stacked]. Neutron scattering experiments were carried out using thermal triple-axis spectrometer Taipan at Australian Centre for Neutron Scattering, ANSTO, Australia. The final energy was fixed as $E_f = 14.8$ meV in energy loss measurement mode ($E = E_i - E_f$), with a pyrolytic graphite filter, a double focusing monochromator, and a vertical focusing analyzer. For example, to measure the excitations at 16 meV, E_i was set as 30.8 meV. The scattering plane $[H, H, L]$ was defined by $\mathbf{Q} = (H, K, L) = (q_xa/2\pi, q_yb/2\pi, q_zc/2\pi)$ in reciprocal lattice unit (r.l.u.) using the tetragonal lattice: $a = b = 3.85$ Å, $c = 30.02$ Å. The total mosaic of our sample mount was about 4.5° both in $[H, H, 0]$ and $[0, 0, L]$ directions. Plane wave pseudopotential based density-functional-theory (DFT) calculations were performed using Quantum ESPRESSO numerical code [44,64].

The 12442-type FeSC $KCa_2Fe_4As_4F_2$ has a layered tetragonal crystal structure (space group $I4/mmm$, No. 139), where the in-plane lattice constant a lies between those of KFe_2As_2 and CaFeAsF, and the c lattice constant is very close to the sum of that of KFe_2As_2 and twice of that of CaFeAsF. Therefore, it can be viewed as an intergrowth of CaFeAsF and KFe_2As_2, where the asymmetric bilayers of Fe_2As_2 are separated by the insulating Ca_2F_2 layers [Fig. 1(e)] [40], much like $Bi_2Sr_2CaCu_2O_{8+\delta}$ (Bi2212) or $YBa_2Cu_3O_{6+\delta}$ (YBCO) [65]. Such structure yields a hole-type self-doping at a level of 0.25 holes/Fe [66], but both the intrabilayer distance and the interbilayer distance are too large to establish a 3D long-range antiferromagnetic order [41,67]. Transport measurements suggest that both normal state and superconducting state are highly anisotropic [42,43,68,69], much like the quasi-2D characteristic in cuprates. Our recent angle-resolved-photoemission-spectroscopy (ARPES) measurements also reveal a clear band splitting effect induced by the interlayer interorbital interactions [70] analogous to the bilayer splitting in Bi2212 [11,71]. While the DFT calculations suggest ten

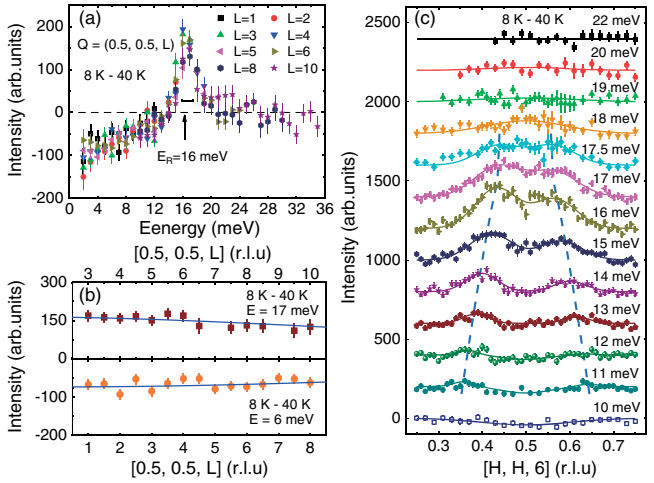

FIG. 2. (a) Spin resonant peak as shown by the difference between $T = 8$ K and 40 K of energy scans at $Q = (0.5, 0.5, L)$ with $L = 1 \sim 10$. (b) L dependence of the intensity gain at $E = 17$ meV and the intensity loss at $E = 6$ meV in the superconducting state. The solid lines represent the square of magnetic form factor $|F(Q)|^2$ after normalizing to the intensity. (c) Constant-energy scans of the intensity difference between $T = 8$ K and 40 K along the $[H, H, 6]$ direction from $E = 10$ meV to 22 meV. All data are shifted by a fixed step for clarity. The solid lines are two-Gaussian-peak fittings, where the data from 18 meV to 20 meV is only fitted by single Gaussian peak. The horizontal bar shows the energy resolution of spectrometer, and all dashed lines are guides to eyes.

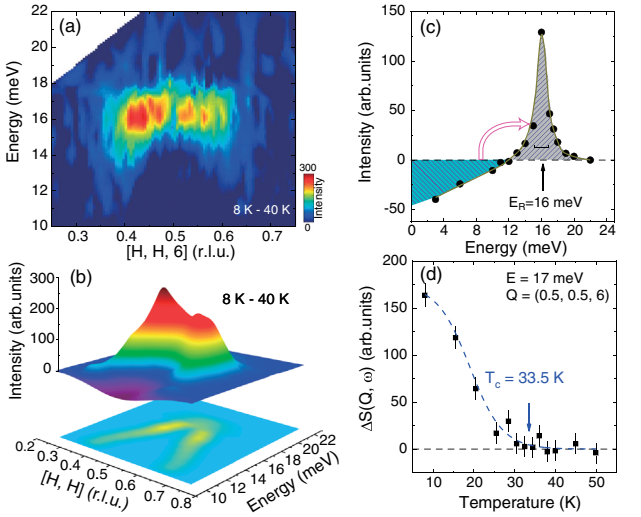

FIG. 3. (a) and (b) 2D color mapping and 3D sketch picture of the spin resonant mode obtained from Fig. 2(c), where a clear downward dispersion is found. (c) Integrated intensity differences between $T = 8$ K and 40 K from 3 meV to 22 meV. The shadow regions suggest similar areas for the intensity gain and loss. (d) Temperature dependence of the spin resonance at $E = 17$ meV and $Q = (0.5, 0.5, 6)$ after subtracting a constant background from 35 to 50 K. The arrow marks the $T_c = 33.5$ K. The horizontal bar shows the energy resolution of spectrometer, and all dashed lines are guides to the eyes.

degenerated bands forming four visible hole pockets with distinct sizes around the Γ point and three small electron pockets around the M point [Fig. 1(f)] [44], three splitting hole pockets and a very tiny electron pocket ($r_\delta \approx 0.04\pi/a$) are also observed by ARPES measurements [70]. All these facts suggest the Fermi surface nesting along the (π, π) direction based on the weak coupling scenario is unlikely to happen in this compound [20–22]. However, according to the strong coupling approach, the $s^{\pm}$-wave pairings with a spin resonance can still occur between the Fermi pockets connected by a longitudinal wave vector Q along the (π, π) direction [Fig. 1(f)] [23–28].

The main results are shown in Figs. 2 and 3. We have performed energy scans at $Q = (0.5, 0.5, L)$ from 2 to 35 meV for $L = 1 \sim 10$ in the $[H, H, L]$ scattering plane. After subtracting the intensity of spin excitations in the normal state ($T = 40$ K), we can identify a spin resonant mode in the superconducting state at $T = 8$ K for a clear spectral-weight gain above 13 meV and a depletion below this energy. The resonant peak has a maximum intensity at $E_R = 16$ meV and a nearly resolution-limited width, and all data are overlapped for different L's [Fig. 2(a)]. Further, L dependence were measured at fixed energies $E = 17$ meV and 6 meV, both of which show no L modulation but simply follow the square of Fe^{2+} magnetic form factor [Fig. 2(b)]. Thus, the resonance is completely 2D, consistent with the transport results for the 2D superconductivity [42,43,68,69], and it also suggests 2D magnetic interactions similar to LaFeAsO [72]. To map out the dispersion of the resonance, we have carried out systematic constant-energy scans along the $[H, H, 6]$ direction from 3 meV to 22 meV. The contamination of the phonon scattering can be removed by the intensity difference between 8 K and 40 K, which clearly reveals two incommensurate resonant peaks along the $[H, H]$ direction in broad widths [Fig. 2(c)]. There is a weak negative intensity difference below 12 meV, but two asymmetric peaks emerge above 11 meV and they quickly increase before finally merging together at 18 meV, then disappear above 20 meV. We demonstrate the spectral-weight gain for the resonance mode in 2D color mapping in Fig. 3(a), where most contributions are from spin excitations around 16 meV, namely, the resonant energy E_R. After applying a two-Gaussian-peak fitting, we obtain an explicit downward dispersion of the resonance with increasing peak width upon increasing energy [Fig. 3(b)]. At 18 meV and 19 meV, we have to use a single Gaussian peak function to fit for the broad and weak intensity. The energy dependence of the integrated intensity from fitting functions is present in Fig. 3(c). The resonant peak is even sharper compared to that in the energy scans and clearly resolution limited. The spectral weight is conserved for nearly identical areas of the negative and positive parts. Figure 3(d) shows the order-parameter-like intensity gain for the resonance at

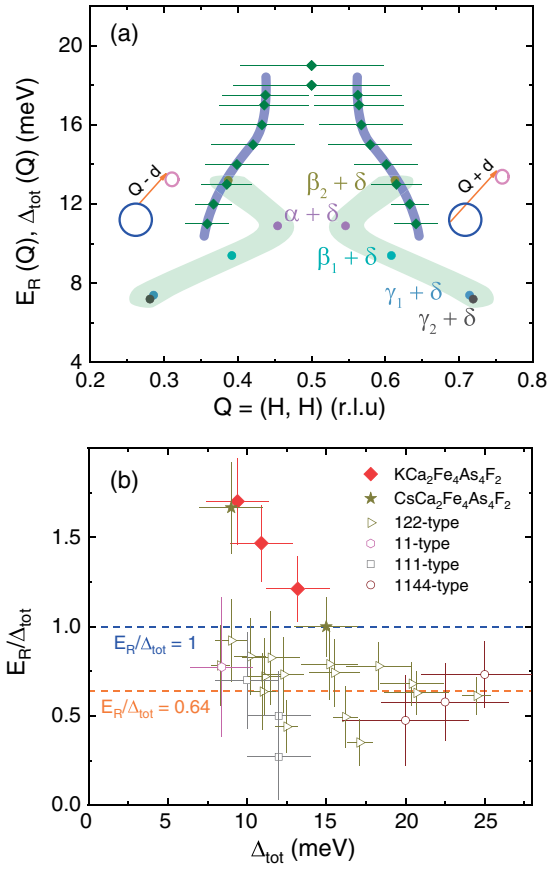

FIG. 4. (a) Comparison between the dispersion of the spin resonance and $\Delta_{tot}(Q)$ in $KCa_2Fe_4As_4F_2$. The gaps are summed on two Fermi pockets linked by longitudinally incommensurate wave vectors $Q + d$ and $Q - d$. The horizontal bars are the peak width obtained from Fig. 2(c). The shadow areas mark the size of electron pocket at the M point [44]. (b) The ratio of E_R/Δ_{tot} in 12442-type FeSCs and other compounds. Here, we use three values of Δ_{tot} for $KCa_2Fe_4As_4F_2$ [$\Delta_{tot} = 13.2$ meV $(\beta_2 + \delta)$, 10.9 meV $(\alpha + \delta)$, 9.4 meV $(\beta_1 + \delta)$ from ARPES results], and two values for $CsCa_2Fe_4As_4F_2$ ($\Delta_L + \Delta_L = 15$ meV and $\Delta_L + \Delta_S = 9$ meV from μSR results).

$E = 17$ meV and $Q = (0.5, 0.5, 6)$, which decreases upon warming up and ceases at $T_c = 33.5$ K.

We further summarize the dispersion of spin resonance and compare with the momentum dependence of $\Delta_{tot}(Q)$ from ARPES results [70] in Fig. 4(a). Here, Δ_{tot} actually has different magnitudes at several incommensurate wave vectors $Q \pm d$ along the $[H, H]$ direction, where the incommensurability d is determined by the mismatched radiuses $\sqrt{r_h^2 - r_e^2}$ [44]. Although an hourglasslike shape of $\Delta_{tot}(Q)$ qualitatively scales with the downward dispersion of the spin resonance, the overall resonant intensities are clearly above Δ_{tot} for most of Q positions, where we could not identify the incommensurability of those resonant peaks above 18 meV for their weak intensities and broadening widths. Such results are apparently inconsistent with the spin-exciton picture under $s^{\pm}$ pairing [29–31]. The resolution-limited peak width of energy dependence together with downward dispersions cannot be explained by the s^{++}-pairing picture [32,34,35], either. Only when the system is proximate to the magnetic quantum critical point (QCP), s^{++} pairing may give a sharp peak of $\chi''(Q, \omega)$ above Δ_{tot} [35]. However, $KCa_2Fe_4As_4F_2$ has a hole concentration similar to the overdoped $Ba_{1-x}K_xFe_2As_2$ and certainly far away from a magnetic instability or QCP [40,66,67], as electron dopings from Co or Ni substitutions cannot induce any magnetic orders but only suppress the T_c [73]. We give a direct comparison between the resonant energy E_R and Δ_{tot} together with other FeSCs in Fig. 4(b) [12,15,39], here we use $\Delta_{tot} = 13.2$ meV $(\beta_2 + \delta)$, 10.9 meV $(\alpha + \delta)$, 9.4 meV $(\beta_1 + \delta)$, respectively. For all cases, we have $E_R/\Delta_{tot} > 1$. Neutron scattering on the powder sample of another 12442-type FeSC $CsCa_2Fe_4As_4F_2$ ($T_c = 28.9$ K) suggests a spin resonance at $E_R = 15$ meV [74], and μSR experiments give two superconducting gaps $\Delta_L = 7.5$ meV and $\Delta_S = 1.5$ meV, resulting in $E_R/\Delta_{tot} \geq 1$, too. Apparently, the large ratio of E_R/Δ_{tot} makes the 12442-type FeSCs different from other systems, where the scaling of $E_R/\Delta_{tot} = 0.64$ holds for most compounds.

Regardless of the abnormal ratio of E_R/Δ_{tot}, the observed spin resonance in $KCa_2Fe_4As_4F_2$ at $Q = (0.5, 0.5)$ [or (π, π)] shares many commonalities with cuprates [10,11,18]. First, the resonant energy $E_R = 16$ meV gives a ratio E_R/k_BT_c of 5.5, larger than those other FeSCs [Fig. 1(e)] [41]. Together with $CsCa_2Fe_4As_4F_2$ and the 112-type FeSC, such a ratio in these materials with 2D spin resonance seems to follow the relation $E_R/k_BT_c = 5.8$ in cuprates [12,41,74]. Second, the 2D nature of the resonant intensity directly responds to the anisotropic superconductivity similar to that in cuprates [11,42,43,68,69]. Because of weak intrabilayer magnetic interactions, a splitting for the odd and even L-modulated resonant modes as found in $CaKFe_4As_4$ and underdoped bilayer cuprates does not appear in this compound [10,39]. Finally, the downward dispersion of the spin resonance mode intimately resembles the lower branch of the hourglass type of spin excitations in hole-doped cuprates [8,10,11]. It should be noticed that a small d-wave gap (< 2 meV) may exist in $KCa_2Fe_4As_4F_2$ as shown by other measurements [75,76], but it cannot cause a downward dispersion of the resonance at high energy. For reference, in the heavily hole overdoped KFe_2As_2 with possible line nodes in the gaps, the spin excitations are incommensurate both at the normal state and superconducting state [77,78]. Furthermore, in a heavy-fermion compound $Ce_{1-x}Yb_xCoIn_5$ with multiband d-wave pairings, an upward-dispersing spin resonance has been revealed, opposite to the case in cuprates, which is argued to be induced by the strong couplings with the 3D spin waves through the hybridization between localized and itinerant electrons [79,80].

In conclusion, the emergence of a 2D spin resonant mode with downward dispersion above Δ_{tot} in $KCa_2Fe_4As_4F_2$

deeply challenges the common understanding of the resonance modes as magnetic excitons regardless of underlining pairing symmetry schemes. Along with previous results like $Ce_{1-x}Yb_xCoIn_5$ [79,80], these counterexamples suggest the spin-exciton scenario of the spin resonance may not be appropriate, when the local moments and itinerant electrons are strongly coupled in the multiband unconventional superconductors. Further theoretical and experimental investigations on the origin of the spin resonance are highly desired in these fascinating compounds concerning the dimensionality of electronic behaviors, and it will certainly inspire the quest for a universal mechanism of the magnetically driven picture of unconventional superconductivity.

This work is supported by the National Key Research and Development Program of China (Grants No. 2018YFA0704200, No. 2017YFA0303100, No. 2017YFA0302900, and No. 2016YFA0300500), the National Natural Science Foundation of China (Grants No. 11822411, No. 11961160699, No. 11874401, No. 11674406, and No. 11674372), the Strategic Priority Research Program (B) of the Chinese Academy of Sciences (CAS) (Grants No. XDB07020300, No. XDB25000000, and No. XDB33000000), and Beijing Natural Science Foundation (Grants No. JQ19002). H. L. and L. Z. are grateful for the support from the Youth Innovation Promotion Association of CAS (Grants No. 2016004 and No. 2017013). A. G. acknowledges Homi Bhaba National Institute at Raja Ramanna Centre for Advanced Technology for financial support.

*slli@iphy.ac.cn
†hqluo@iphy.ac.cn

[1] J. Rossat-Mignod, L. P. Regnault, C. Vettier, P. Bourges, P. Burlet, J. Bossy, J. Y. Henry, and G. Lapertot, Physica (Amsterdam) **185C**, 86 (1991).
[2] H. A. Mook, M. Yethiraj, G. Aeppli, T. E. Mason, and T. Armstrong, Phys. Rev. Lett. **70**, 3490 (1993).
[3] N. K. Sato, N. Aso, K. Miyake, R. Shiina, P. Thalmeier, G. Varelogiannis, C. Geibel, F. Steglich, P. Fulde, and T. Komatsubara, Nature (London) **410**, 340 (2001).
[4] C. Stock, C. Broholm, J. Hudis, H. J. Kang, and C. Petrovic, Phys. Rev. Lett. **100**, 087001 (2008).
[5] A. D. Christianson, E. A. Goremychkin, R. Osborn, S. Rosenkranz, M. D. Lumsden, C. D. Malliakas, I. S. Todorov, H. Claus, D. Y. Chung, M. G. Kanatzidis, R. I. Bewley, and T. Guidi, Nature (London) **456**, 930 (2008).
[6] T. J. Liu, J. Hu, B. Qian, D. Fobes, Z. Q. Mao, W. Bao, M. Reehuis, S. A. J. Kimber, K. Prokes, S. Matas, D. N. Argyriou, A. Hiess, A. Rotaru, H. Pham, L. Spinu, Y. Qiu, V. Thampy, A. T. Savici, J. A. Rodriguez, and C. Broholm, Nat. Mater. **9**, 718 (2010).
[7] D. S. Inosov, J. T. Park, P. Bourges, D. L. Sun, Y. Sidis, A. Schneidewind, K. Hradil, D. Haug, C. T. Lin, B. Keimer, and V. Hinkov, Nat. Phys. **6**, 178 (2010).
[8] J. M. Tranquada, G. Xu, and I. A. Zaliznyak, J. Magn. Magn. Mater. **350**, 148 (2014).
[9] P. Dai, Rev. Mod. Phys. **87**, 855 (2015).
[10] Y. Sidis, S. Pailhès, V. Hinkov, B. Fauqué, C. Ulrich, L. Capogna, A. Ivanov, L.-P. Regnault, B. Keimer, and P. Bourges, C. R. Phys. **8**, 745 (2007).
[11] M. Eschrig, Adv. Phys. **55**, 47 (2006).
[12] G. Yu, Y. Li, E. M. Motoyama, and M. Greven, Nat. Phys. **5**, 873 (2009).
[13] M. Wang, H. Luo, J. Zhao, C. Zhang, M. Wang, K. Marty, S. Chi, J. W. Lynn, A. Schneidewind, S. Li, and P. Dai, Phys. Rev. B **81**, 174524 (2010).
[14] J. T. Park, D. S. Inosov, A. Yaresko, S. Graser, D. L. Sun, P. Bourges, Y. Sidis, Y. Li, J.-H. Kim, D. Haug, A. Ivanov, K. Hradil, A. Schneidewind, P. Link, E. Faulhaber, I. Glavatskyy, C. T. Lin, B. Keimer, and V. Hinkov, Phys. Rev. B **82**, 134503 (2010).
[15] D. S. Inosov, J. T. Park, A. Charnukha, Y. Li, A. V. Boris, B. Keimer, and V. Hinkov, Phys. Rev. B **83**, 214520 (2011).
[16] P. D. Johnson, G. Xu, and W. Yin, *Iron-Based Superconductivity* (Springer, New York, 2015), Chap. 5.
[17] P. Monthoux, D. Pines, and G. G. Lonzarich, Nature (London) **450**, 1177 (2007).
[18] D. J. Scalapino, Rev. Mod. Phys. **84**, 1383 (2012).
[19] Q. Si, R. Yu, and E. Abrahams, Nat. Rev. Mater. **1**, 16017 (2016).
[20] P. Richard, T. Sato, K. Nakayama, T. Takahashi, and H. Ding, Rep. Prog. Phys. **74**, 124512 (2011).
[21] A. V. Chubukov, D. V. Efremov, and I. Eremin, Phys. Rev. B **78**, 134512 (2008).
[22] I. Mazin and J. Schmalian, Physica (Amsterdam) **469C**, 614 (2009).
[23] K. Seo, B. A. Bernevig, and J. Hu, Phys. Rev. Lett. **101**, 206404 (2008).
[24] P. J. Hirschfeld, M. M. Korshunov, and I. I. Mazin, Rep. Prog. Phys. **74**, 124508 (2011).
[25] F. Wang and D. H. Lee, Science **332**, 200 (2011).
[26] M. M. Korshunov and I. Eremin, Phys. Rev. B **78**, 140509 (R) (2008).
[27] M. M. Parish, J. Hu, and B. A. Bernevig, Phys. Rev. B **78**, 144514 (2008).
[28] T. A. Maier and D. J. Scalapino, Phys. Rev. B **78**, 020514(R) (2008).
[29] T. A. Maier, S. Graser, D. J. Scalapino, and P. Hirschfeld, Phys. Rev. B **79**, 134520 (2009).
[30] T. Das and A. V. Balatsky, Phys. Rev. Lett. **106**, 157004 (2011).
[31] M. G. Kim, G. S. Tucker, D. K. Pratt, S. Ran, A. Thaler, A. D. Christianson, K. Marty, S. Calder, A. Podlesnyak, S. L. Budko, P. C. Canfield, A. Kreyssig, A. I. Goldman, and R. J. McQueeney, Phys. Rev. Lett. **110**, 177002 (2013).
[32] S. Onari, H. Kontani, and M. Sato, Phys. Rev. B **81**, 060504 (R) (2010).
[33] S. Onari and H. Kontani, Phys. Rev. Lett. **109**, 137001 (2012).
[34] H. Kontani and S. Onari, Phys. Rev. Lett. **104**, 157001 (2010).
[35] L. Takeuchi, Y. Yamakawa, and H. Kontani, Phys. Rev. B **98**, 165143 (2018).

[36] C. Zhang, H.-F. Li, Y. Song, Y. Su, G. Tan, T. Netherton, C. Redding, S. V. Carr, O. Sobolev, A. Schneidewind, E. Faulhaber, L. W. Harriger, S. Li, X. Lu, D.-X. Yao, T. Das, A. V. Balatsky, Th. Brückel, J. W. Lynn, and P. Dai, Phys. Rev. B **88**, 064504 (2013).

[37] D. Hu, Z. Yin, W. Zhang, R. A. Ewings, K. Ikeuchi, M. Nakamura, B. Roessli, Y. Wei, L. Zhao, G. Chen, S. Li, H. Luo, K. Haule, G. Kotliar, and P. Dai, Phys. Rev. B **94**, 094504 (2016).

[38] R. Zhang, W. Wang, T. A. Maier, M. Wang, M. B. Stone, S. Chi, B. Winn, and P. Dai, Phys. Rev. B **98**, 060502(R) (2018).

[39] T. Xie, Y. Wei, D. Gong, T. Fennell, U. Stuhr, R. Kajimoto, K. Ikeuchi, S. Li, J. Hu, and H. Luo, Phys. Rev. Lett. **120**, 267003 (2018).

[40] Z. Wang, C. He, S. Wu, Z. Tang, Y. Liu, A. Ablimit, C. Feng, and G. Cao, J. Am. Chem. Soc. **138**, 7856 (2016).

[41] T. Xie, D. Gong, H. Ghosh, A. Ghosh, M. Soda, T. Masuda, S. Itoh, F. Bourdarot, L.-P. Regnault, S. Danilkin, S. Li, and H. Luo, Phys. Rev. Lett. **120**, 137001 (2018).

[42] T. Wang, J. Chu, H. Jin, J. Feng, L. Wang, Y. Song, C. Zhang, X. Xu, W. Li, Z. Li, T. Hu, D. Jiang, W. Peng, X. Liu, and G. Mu, J. Phys. Chem. C **123**, 13925 (2019).

[43] T. Wang, C. Zhang, L. C. Xu, J. H. Wang, S. Jiang, Z. W. Zhu, Z. S. Wang, J. N. Chu, J. X. Feng, L. L. Wang, W. Li, T. Hu, X. S. Liu, and G. Mu, Sci. China Phys. Mech. Astron. **63**, 227412 (2020).

[44] See Supplemental Material at http://link.aps.org/supplemental/10.1103/PhysRevLett.125.117002 for the sample characterization, raw data of neutron scattering experiments and DFT calculations on the band structure and Fermi surfaces, which includes Refs. [45–63].

[45] H. Jiang, Y. Sun, Z. Xu, and G. Cao, Chin. Phys. B **22**, 087410 (2013).

[46] Z.-C. Wang, C.-Y. He, S.-Q. Wu, Z.-T. Tang, Y. Liu, A. Ablimit, Q. Tao, C.-M. Feng, Z.-A. Xu, and G.-H. Cao, J. Phys. Condens. Matter **29**, 11LT01 (2017).

[47] Z.-C. Wang, C.-Y. He, S.-Q. Wu, Z.-T. Tang, Y. Liu, and G.-H. Cao, Chem. Mater. **29**, 1805 (2017).

[48] S.-Q. Wu, Z.-C. Wang, C.-Y. He, Z.-T. Tang, Y. Liu, and G.-H. Cao, Phys. Rev. Mater. **1**, 044804 (2017).

[49] A. Iyo, K. Kawashima, T. Kinjo, T. Nishio, S. Ishida, H. Fujihisa, Y. Gotoh, K. Kihou, H. Eisaki, and Y. Yoshida, J. Am. Chem. Soc. **138**, 3410 (2016).

[50] W. R. Meier, T. Kong, S. L. Bud'ko, and P. C. Canfield, Phys. Rev. Mater. **1**, 013401 (2017).

[51] J. Bao, K. Willa, M. P. Smylie, H. Chen, U. Welp, D. Y. Chung, and M. G. Kanatzidis, Cryst. Growth Des. **18**, 3517 (2018).

[52] F. Han, X. Zhu, G. Mu, P. Cheng, and H.-H. Wen, Phys. Rev. B **78**, 180503(R) (2008).

[53] M. Tegel, S. Johansson, V. Weiß, I. Schellenberg, W. Hermes, R. Pöttgen, and D. Johrendt, Europhys. Lett. **84**, 67007 (2008).

[54] X. Zhu, F. Han, P. Cheng, G. Mu, B. Shen, L. Fang, and H.-H. Wen, Europhys. Lett. **85**, 17011 (2009).

[55] X. Zhu, F. Han, P. Cheng, G. Mu, B. Shen, B. Zeng, and H.-H. Wen, Physica (Amsterdam) **469C**, 381 (2009).

[56] S. Matsuishi, Y. Inoue, T. Nomura, H. Yanagi, M. Hirano, and H. Hosono, J. Am. Chem. Soc. **130**, 14428 (2008).

[57] Y. Xiao, Y. Su, R. Mittal, T. Chatterji, T. Hansen, C. M. N. Kumar, S. Matsuishi, H. Hosono, and Th. Brueckel, Phys. Rev. B **79**, 060504(R) (2009).

[58] H. Chen, Y. Ren, Y. Qiu, W. Bao, R. H. Liu, G. Wu, T. Wu, Y. L. Xie, X. F. Wang, Q. Huang, and X. H. Chen, Europhys. Lett. **85**, 17006 (2009).

[59] J. K. Dong, S. Y. Zhou, T. Y. Guan, H. Zhang, Y. F. Dai, X. Qiu, X. F. Wang, Y. He, X. H. Chen, and S. Y. Li, Phys. Rev. Lett. **104**, 087005 (2010).

[60] P. Dai, J. Hu, and E. Dagotto, Nat. Phys. **8**, 709 (2012).

[61] W. R. Meier, Q.-P. Ding, A. Kreyssig, S. L. Budko, A. Sapkota, K. Kothapalli, V. Borisov, R. Valent, C. D. Batista, P. P. Orth, R. M. Fernandes, A. I. Goldman, Y. Furukawa, A. E. Böhmer, and P. C. Canfield, npj Quantum Mater. **3**, 5 (2018).

[62] A. Kreyssig, J. M. Wilde, A. E. Böhmer, W. Tian, W. R. Meier, B. Li, B. G. Ueland, M. Xu, S. L. Bud'ko, P. C. Canfield, R. J. McQueeney, and A. I. Goldman, Phys. Rev. B **97**, 224521 (2018).

[63] J. C. Stewart, D. S. Matthew, J. P. Chris, J. H. Phil, I. J. P. Matt, R. Keith, and C. P. Mike, Z. Kristallogr. **220**, 567 (2005).

[64] P. Giannozzi, S. Baroni, N. Bonini, M. Calandra, R. Car, C. Cavazzoni *et al.*, J. Phys. Condens. Matter **21**, 395502 (2009).

[65] B. Raveau, C. Michel, M. Hervieu, and D. Groult, *Crystal Chemistry of High-T_cSuperconducting Copper Oxides* (Springer Press, New York, 2015), Vol. 15.

[66] G. Wang, Z. Wang, and X. Shi, Europhys. Lett. **116**, 37003 (2016).

[67] Z. Wang, C. He, Z. Tang, S. Wu, and G. Cao, Sci. China Mater. **60**, 83 (2017).

[68] A. B. Yu, T. Wang, Y. F. Wu, Z. Huang, H. Xiao, G. Mu, and T. Hu, Phys. Rev. B **100**, 144505 (2019).

[69] Z. C. Wang, Y. Liu, S. Q. Wu, Y. T. Shao, Z. Ren, and G. H. Cao, Phys. Rev. B **99**, 144501 (2019).

[70] D. Wu, W. Hong, C. Dong, X. Wu, Q. Sui, J. Huang *et al.*, Phys. Rev. B **101**, 224508 (2020).

[71] D. L. Feng, N. P. Armitage, D. H. Lu, A. Damascelli, J. P. Hu, P. Bogdanov, A. Lanzara, F. Ronning, K. M. Shen, H. Eisaki, C. Kim, J.-i. Shimoyama, K. Kishio, and Z.-X. Shen, Phys. Rev. Lett. **86**, 5550 (2001).

[72] M. Ramazanoglu, J. Lamsal, G. S. Tucker, J.-Q. Yan, S. Calder, T. Guidi, T. Perring, R. W. McCallum, T. A. Lograsso, A. Kreyssig, A. I. Goldman, and R. J. McQueeney, Phys. Rev. B **87**, 140509(R) (2013).

[73] J. Ishida, S. Iimura, and H. Hosono, Phys. Rev. B **96**, 174522 (2017).

[74] D. T. Adroja, S. J. Blundell, F. Lang, H. Luo, Z. Wang, and G. Cao, J. Phys. Condens. Matter **32**, 435603 (2020).

[75] M. Smidman, F. K. K. Kirschner, D. T. Adroja, A. D. Hillier, F. Lang, Z. C. Wang, G. H. Cao, and S. J. Blundell, Phys. Rev. B **97**, 060509(R) (2018).

[76] T. Wang, J. Chu, J. Feng, L. Wang, X. Xu, W. Li, H.-H. Wen, X. Liu, and G. Mu, Sci. China Phys. Mech. Astron. **63**, 297412 (2020).

[77] C. H. Lee, K. Kihou, H. Kawano-Furukawa, T. Saito, A. Iyo, H. Eisaki, H. Fukazawa, Y. Kohori, K. Suzuki, H. Usui, K. Kuroki, and K. Yamada, Phys. Rev. Lett. **106**, 067003 (2011).

[78] S. Shen, X. Zhang, H. Wo, Y. Shen, Y. Feng, A. Schneidewind, P. Cermak, W. Wang, and J. Zhao, Phys. Rev. Lett. **124**, 017001 (2020).

[79] Y. Song, J. Van Dyke, I. K. Lum, B. D. White, S. Jang, D. Yazici, L. Shu, A. Schneidewind, P. Čermák, Y. Qiu, M. B. Maple, D. K. Morr, and P. Dai, Nat. Commun. **7**, 12774 (2016).

[80] Y. Song, W. Wang, J. S. Van Dyke, N. Pouse, S. Ran, D. Yazici, A. Schneidewind, P. Čermák, Y. Qiu, M. B. Maple, D. K. Morr, and P. Dai, Commun. Phys. **3**, 98 (2020).